

PAPER • OPEN ACCESS

## Study on Ground Simulation Loading System of a Carrier Rudder Surface

To cite this article: Minbo Yang *et al* 2019 *IOP Conf. Ser.: Mater. Sci. Eng.* **563** 042036

View the [article online](#) for updates and enhancements.



**IOP | ebooks™**

Bringing you innovative digital publishing with leading voices to create your essential collection of books in STEM research.

Start exploring the collection - download the first chapter of every title for free.

# Study on Ground Simulation Loading System of a Carrier Rudder Surface

Minbo Yang<sup>1,a</sup>, Yueyue Ji<sup>2</sup>, Ming Ji<sup>1</sup>, Long Shui<sup>1</sup> and Zhaohui Fu<sup>1</sup>

<sup>1</sup>Lanzhou Institute of Physics, Lanzhou, Gansu, China

<sup>2</sup>Lanzhou Vocationnal College of Science & Technology, Lanzhou, Gansu, China

<sup>a</sup> Corresponding author: yangminbo1119@126.com

**Abstract.** Aimed at the requirement that the rudder surface of a carrier has a large rotary inertia and a large constant load, the existing loading methods can not meet the loading requirement, so a new type of loading system is designed. This paper introduces the structure and working principle of the system in detail. At the same time, the main parameters of the system are calculated. Then the loading result is simulated and analyzed by using the MATLAB/Simulink. Finally, the ground loading experiment is carried out. The experiment result shows that the experiment result of the loading system is consistent with the simulation result, so the loading system is accurate.

## 1. Introduction

In recent years, with the rapid development of the world's space industry, space launch activities are becoming increasingly frequent, so how to reduce the cost of space launch has gradually become a common concern of all countries in the world [1]. At present, the cost of launching is reduced mainly through the research on the recovery and reuse technology of carrier at home and abroad [2]. Because the rudder surface of a carrier will be affected by wind load during its flight from initial folding and locking state to unfolding state, it is necessary to assess the rudder surface performance by ground simulation loading experiment before flight experiment. In the past, the ground simulation loading experiment for a carrier rudder surface was carried out by means of motor loading. Because of the large rotary inertia of the rudder surface and the large load of the rudder surface, it produces a large additional inertia torque in the course of rudder surface rotation. The control law of the motor loading system can not completely eliminate the additional inertia torque, so that the loading error of the motor loading system reaches 35% at the end of the rotation, which results in that the loading error is too large. At present, there are three main methods of ground simulation loading: motor loading method [3], air cylinder loading method [4], and wind tunnel loading method [5], among which the wind tunnel loading method needs to be carried out in a professional aerodynamic institute and the price is very expensive. Because of the movement of the piston rod in the air cylinder loading method, which will change the air cylinder volume, the pressure in the cylinder cavity will also change accordingly. Thus the existing loading methods can not meet the constant load requirement of a carrier rudder surface.

To solve this problem, a new type of loading system is designed. The system exerts the load torque to the rudder surface by loading fork. When simulating the upwind load, the air cylinder makes the loading fork output an opposite direction load torque to the rotation direction of the rudder surface by the turntable. When simulating downwind load, through changing twining direction of wire rope on



turntable, the air cylinder makes the loading fork output a same direction load torque to the rotation direction of the rudder surface by the turntable. The load torque can be adjusted by adjusting the initial air pressure in the air cylinder cavity. The initial volume of the air cylinder is greatly enlarged by increasing the air vessel in the system. The variation of the volume produced by the movement of the piston rod is much smaller than the volume of the air vessel, so the loading system can exert constant load. Then the loading result is simulated and analyzed by using the MATLAB/Simulink. Finally, the ground simulation loading experiment is carried out, and the experiment result shows that the experiment result is consistent with the simulation result, so the loading system is accurate.

## 2. Structure and composition of the loading system

The loading system consists of loading fork, rotating shaft, turntable, screw rod, wire rope, air cylinder, air vessel, bracket, pressure sensor, high speed photography, pressure gauge, air compressor, and IPC etc. The schematic diagram of the loading system is shown in Figure 1, and the physical diagram is shown in Figure 2.

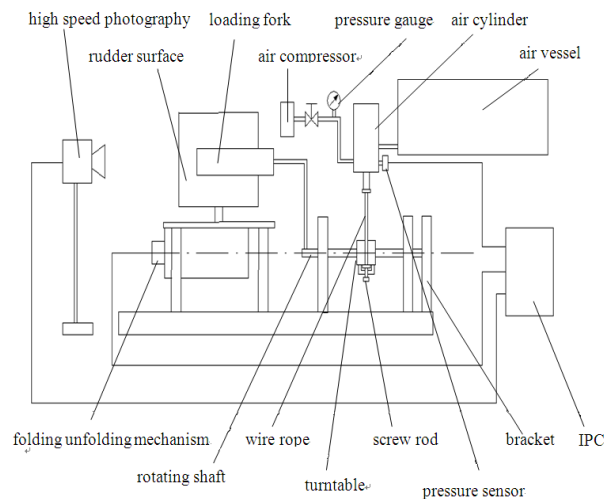


Figure 1. The schematic diagram of the loading system



Figure 2. The physical diagram of the loading system

## 3. Working principle

At the beginning of the experiment, the certain amount of air is filled into the air cylinder and air vessel through the air compressor. The air cylinder is connected with the air vessel through the pipeline. At this time the output of the air cylinder is tension. A pressure sensor is installed on the air cylinder to measure the pressure of the air cylinder cavity in real time during the experiment and transmit the data to the IPC. The piston rod of the air cylinder is connected with the turntable by wire rope. The movement direction of the wire rope is always the tangent direction of the turntable. The screw rod tightens the wire rope in the V-groove of the turntable. The wire rope drives the turntable to rotate. The force direction of the turntable can be changed by changing the twining direction of the wire rope on the turntable. The turntable and rotating shaft are installed on the experiment bench

through the bracket. The axis of the turntable and the axis of the rotating shaft are coaxial. There is a spline connection between the rotating shaft and the loading fork arm. There is a bolt connection between the rudder surface and the loading fork. The axis of the rudder surface and the axis of the rotating shaft are coaxial. When simulating the upwind load, the air cylinder makes the loading fork output an opposite direction load torque to the rotation direction of the rudder surface by the turntable. When simulating downwind load, through changing twining direction of wire rope on turntable, the air cylinder makes the loading fork output a same direction load torque to the rotation direction of the rudder surface by the turntable. The load torque can be adjusted by adjusting the initial inflation pressure in the air cylinder cavity. The rotation of rudder surface is accomplished by folding unfolding mechanism. a fire actuator is the power source of folding unfolding mechanism. When the actuator receives the ignition instruction from the IPC, it starts to unfold the rudder surface from 0 ° to 90 °. Load torque of the rudder surface is exerted by loading fork in the course of rudder surface rotation. When the IPC gives the ignition instruction to the actuator, it also gives the trigger instruction to the high speed photography. After receiving the trigger instruction, the high speed photography starts to capture the video information of the rudder surface rotation. After the experiment, the high speed photography outputs the angle-time curve of the rudder surface and the velocity-time curve of the rudder surface. The IPC outputs pessure-time curve of the air cylinder cavity.

#### 4. Principle analysis of constant load loading

When the working process of the air cylinder is isothermal and the air cylinder is not connected to the air vessel, the ideal gas law can be expressed by formula (1)[6].

$$p_1V_1 = p_2V_2 \quad (1)$$

In the formula:

$p_1$ —the pressure of compressed air in the air cylinder cavity when the piston rod is in its initial position, MPa;

$V_1$ —the volume of compressed air in the air cylinder cavity when the piston rod is in its initial position, mm<sup>3</sup>;

$p_2$ —the pressure of compressed air in the cylinder cavity after a certain displacement of piston rod, MPa;

$V_2$ —the volume of compressed air in the air cylinder cavity after a certain displacement of piston rod, mm<sup>3</sup>.

When the air cylinder is connected to the air vessel, the ideal gas law under isothermal condition can be expressed by formula (2).

$$p_1(V_1 + V_0) = p_1(V_2 + V_0 + \Delta V) = p_2(V_2 + V_0) \quad (2)$$

In the formula:

$p_1$ —the pressure of compressed air in the air cylinder cavity when the piston rod is in its initial position, MPa;

$V_1$ —the volume of compressed air in the air cylinder cavity when the piston rod is in its initial position, mm<sup>3</sup>;

$V_0$ —the volume of compressed air in the air vessel cavity, mm<sup>3</sup>;

$V_2$ —the volume of compressed air in the air cylinder cavity after a certain displacement of piston rod, mm<sup>3</sup>;

$\Delta V$ —the variation of the volume produced by the movement of the piston rod, mm<sup>3</sup>.

$p_2$ —the pressure of compressed air in the cylinder cavity after a certain displacement of piston rod, MPa.

Because  $\Delta V$  is less than  $V_1$  and  $V_1$  is much less than  $V_0$ , therefore  $\Delta V$  is much less than  $V_0$  and also much less than the sum of  $V_2$  and  $V_0$ , so  $\Delta V$  can be neglected in calculation. Thus we can get that  $p_1$  is approximately equal to  $p_2$  and the loading system can exert the constant load.

## 5. Calculation of main parameters

The main parameters of the loading system are the tightening torque of the screw rod, the minimum diameter of the wire rope, the initial air pressure of the air cylinder cavity and the volume of the air vessel cavity.

### 5.1. Calculation of tightening torque of screw rod

The screw rod tightens the wire rope in the V-groove of the turntable, as shown in Figure 3.

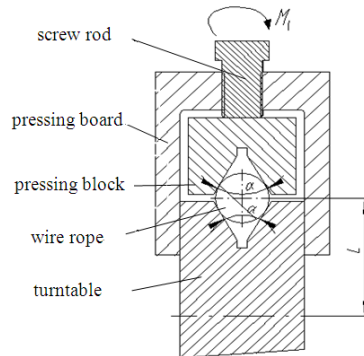


Figure 3. Connection structure between wire rope and turntable

The wire rope should not be loosened during loading, otherwise it will affect the authenticity of loading, which requires sufficient friction between the wire rope and the turntable V-groove. The magnitude of friction is mainly related to the tightening torque of the screw rod, so it is necessary to calculate the tightening torque of the screw rod. During the experiment, the operator exerts the tightening torque to the screw rod by the torque wrench. The tightening torque can be calculated according to formula (3).

$$M_1 = \frac{M_2 d n_1 (\tan \theta - \mu_1)}{4l \mu_2 \cos(90^\circ - \frac{\alpha}{2}) (1 + \mu_1 \tan \theta)} \quad (3)$$

In the formula:

$M_1$ —the tightening torque of the screw rod, N.m;

$M_2$ —the constant load of the rudder surface, N.m;

$d$ —the middle diameter of the screw rod, mm;

$n_1$ —the safety factor, 1.5~2;

$\theta$ —the helix angle of the screw rod, °;

$\mu_1$ —the friction factor between the screw rod and the pressing board, 0.15;

$l$ —the center distance between the wire rope and the turntable, mm;

$\mu_2$ —the friction factor between the wire rope and the turntable V-groove, 0.20;

$\alpha$ —the included angle of the turntable V-groove, °.

### 5.2. Calculation of minimum diameter of wire rope

The steel core wire rope is used in the loading system [7]. Its main function is to transfer the tension of the air cylinder to the turntable. The wire rope bears large tension during working, which belongs to the main stressed component. The minimum diameter of the wire rope can be calculated according to formula (4).

$$d_1 = \sqrt{\frac{4n_2 M_2}{\pi k l \omega \sigma_b}} \quad (4)$$

In the formula:

$d_1$ —the minimum diameter of the screw rod, mm;

$n_2$ —the safety factor, 6~10;

- $M_2$ —the constant load of the rudder surface, N.m;  
 $k$ —the reduction factor, 0.82;  
 $l$ —the center distance between the wire rope and the turntable, mm;  
 $\omega$ —the filling factor of steel wire, 0.46;  
 $\sigma_b$ —the nominal tensile strength of steel wire, MPa.

### 5.3. Calculation of initial air pressure of air cylinder cavity

The air cylinder is the power source of the whole loading system and its internal structure is shown in Figure 4.

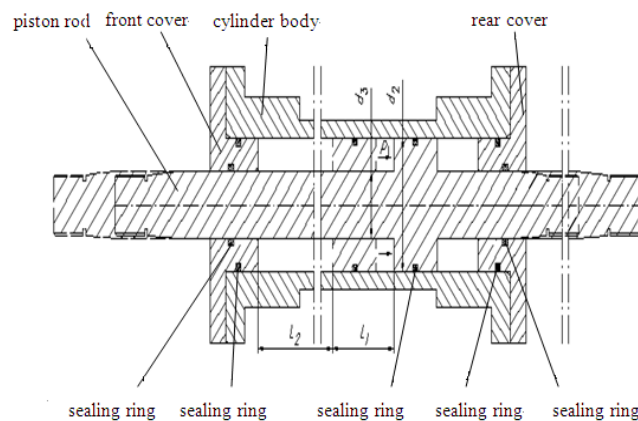


Figure 4. Internal structure of the air cylinder

The load torque exerted by the loading system is related to the initial inflating pressure of the air cylinder cavity. Therefore, the initial inflating pressure of the cylinder cavity should be calculated firstly. The initial inflating pressure of the air cylinder cavity can be calculated according to formula (5).

$$p_1 = \frac{4M_2}{\pi l(d_2^2 - d_3^2)} \quad (5)$$

In the formula:

- $p_1$ —the initial inflating pressure of the air cylinder cavity, MPa;  
 $M_2$ —the constant load of the rudder surface, N.m;  
 $l$ —the center distance between the wire rope and the turntable, mm;  
 $d_2$ —the large end diameter of the piston rod, mm;  
 $d_3$ —the small end diameter of the piston rod, mm.

### 5.4. Calculation of volume of air vessel cavity

The role of air vessel in loading system is to enlarge the volume of air cylinder cavity. The larger the volume of air vessel cavity is, the higher the loading accuracy of loading system is. However, the larger the volume of air vessel cavity is, the longer the inflating time of loading system will be [8]. The long time for inflating is not allowed in high and low temperature experiment. The volume of air vessel cavity can be calculated according to formula (6).

$$V_0 = \frac{\pi(d_2^2 - d_3^2)(l_1 - \eta l_2)}{4\eta} \quad (6)$$

In the formula:

- $V_0$ —the volume of the air vessel cavity, mm<sup>3</sup>;  
 $d_2$ —the large end diameter of the piston rod, mm;  
 $d_3$ —the small end diameter of the piston rod, mm;  
 $l_1$ —the distance of piston rod from initial position to final position, mm;

$\eta$ —the loading error of the loading system, 0.01~0.1;

$l_2$ —the distance of piston rod from final position to front cover of air cylinder, mm.

### 6. Simulation and analysis

Simulation is an important part of product design and it is of great significance to save cost. The loading result should be simulated by using the MATLAB/Simulink before ground experiment [9].

The working process of rudder surface includes static stage and rotation stage. Static stage is the stage from the ignition of actuator to the beginning of rudder surface rotation. Rotation stage is the stage from the beginning of rudder surface rotation to the ending of rudder surface rotation. The simulation model of the static stage is shown in Figure 5, the simulation model of the rotation stage is shown in Figure 6, and the input of the load torque is shown in Figure 7.

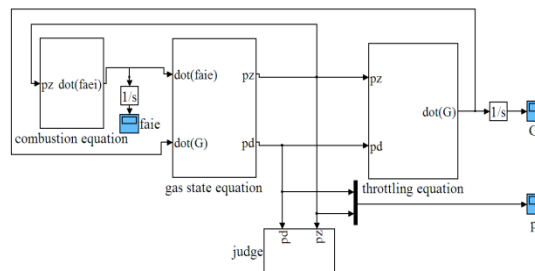


Figure 5. The simulation model of the static stage

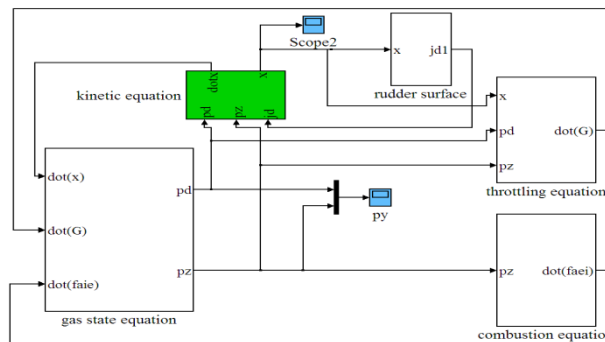


Figure 6. The simulation model of the rotation stage

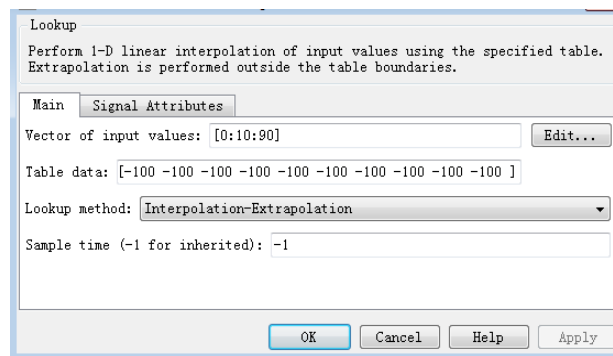


Figure 7. The input of the load torque

The simulation result of rudder surface rotating from 0° to 90° under 100 N.m upwind load can be obtained by running program. The angle-time curve of rudder surface is shown in Figure 8, and the velocity-time curve of rudder surface is shown in Figure 9. According to the simulation curve, the arrival time of rudder surface is 0.672 s and the arrival velocity is 8.3 rad/s.

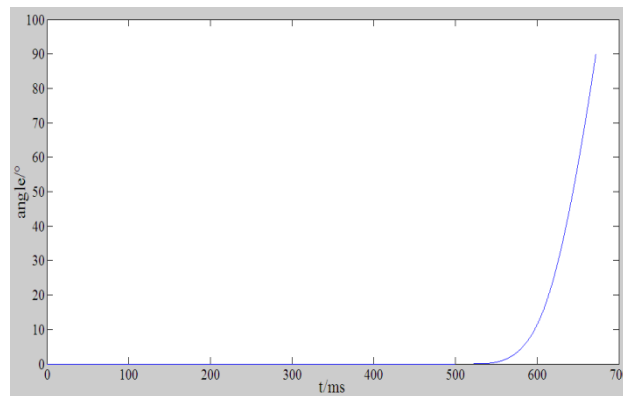


Figure 8. The angle-time curve of rudder surface

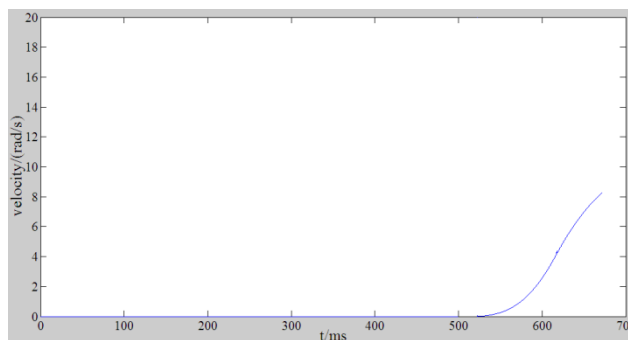


Figure 9. The velocity-time curve of rudder surface

## 7. Verification of ground experiment

The known main experimental parameters are as follows: the middle diameter  $d$  is 10.3 mm, the safety factor  $n_1$  is 1.5, the helix angle  $\theta$  is  $35^\circ$ , the friction factor  $\mu_1$  is 0.15, the center distance  $l$  is 30 mm, the friction factor  $\mu_2$  is 0.2, the included angle  $\alpha$  is  $60^\circ$ , the safety factor  $n_2$  is 10, the reduction factor  $k$  is 0.82, the filling factor  $\omega$  is 0.46, the nominal tensile strength  $\sigma_b$  is 1570 MPa, the large end diameter  $d_2$  is 60 mm, the small end diameter  $d_3$  is 30 mm, the distance  $l_1$  is 48 mm, the loading error  $\eta$  is 0.01, and the distance  $l_2$  is 52 mm.

The main experimental parameters obtained by calculation are as follows: the tightening torque  $M_1$  is 64 N.m, the minimum diameter  $d_1$  is 8.5 mm, the diameter of wire rope in loading system is 13 mm, the initial inflating pressure  $p_1$  is 1.5 MPa, and the volume  $V_0$  is  $1 \times 10^7 \text{ mm}^3$ .

After the experiment is completed, the experiment curves are output by high-speed photography and IPC. The angle-time curve of rudder surface is shown in Figure 10, the velocity-time curve of rudder surface is shown in Figure 11, and the pressure-time curve of the air cylinder cavity is shown in Figure 12.

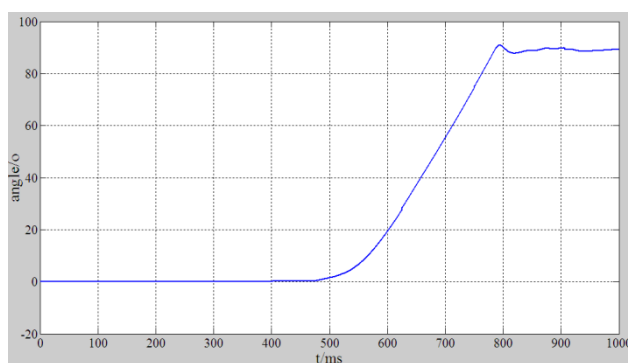


Figure 10. The angle-time curve of rudder surface

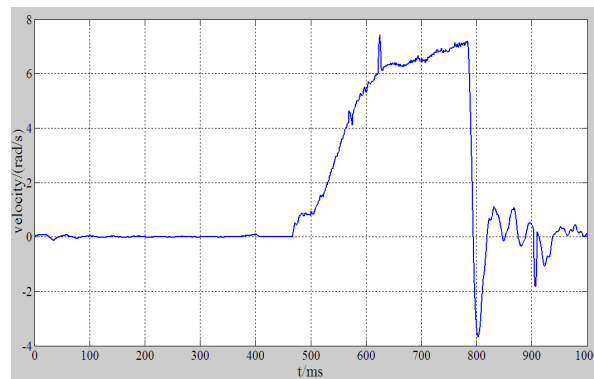


Figure 11. The velocity-time curve of rudder surface

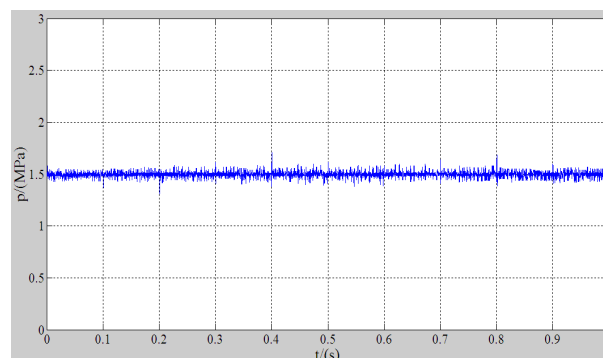


Figure 12. The pressure-time curve of the air cylinder cavity

According to the experiment curves, the arrival time of rudder surface is 0.785 s and the arrival velocity of rudder surface is 7.0 rad/s. By comparing the experimental result with the simulation result, the difference of the arrival time is only 0.113 s, and the difference of the arrival velocity is only 1.3 rad/s. The experimental result is consistent with the simulation result. In addition, according to Figure 12, it can be obtained that the pressure of the air cylinder cavity remains about 1.5 MPa during the working process, so the loading system is accurate.

## 8. Conclusion

According to the loading requirement of a carrier rudder surface, a ground simulation loading system is designed. This paper introduces its composition, working principle and calculation method of main parameters. Then the loading result is simulated and analyzed by using the MATLAB/Simulink. Finally, the ground loading experiment is carried out. The experiment result is consistent with the simulation result, so the loading system is accurate. The system can meet the loading requirement of a carrier rudder surface.

## References

- [1] W. Huang, *Spacecraft Recovery & Remote Sensing*, **38**, 1-12 (2017)
- [2] X. Zheng, Y. Yang, S.D. Yao, *Missiles and Space Vehicles*, 39-46 (2016)
- [3] Y. Rui, J.L. Wei, J. Yan, *Journal of Northwestern Polytechnical University*, **36**, 246-250 (2018)
- [4] J. Li, *Hydraulics Pneumatics & Seals*, **37**, 69-73 (2017)
- [5] W. Song, W. Lu, Z.H. Jiang, *Journal of Experiments in Fluid Mechanics*, **31**, 45-50 (2017)
- [6] L.X. Wu, F.J.Zha, *Journal of Anqing Normal University (Natural Science Edition)*, **22**, 100-102 (2016)
- [7] X.L. Ji, H.F. Li, P.F. Gao, *Hoisting and Conveying Machinery*, 41-43 (2016)
- [8] J.G. Zhang, J. Wang, G.W. Wang, *Ship & Ocean Engineering*, **46**, 134-136 (2017)
- [9] S. Zhao, Y.J. Wei, Y. Guo, *PC Fan*, 178 (2017)
- [10] L. Shui, Y.X. Liu, Y. Yang, *Manned Spaceflight*, **22**, 104-111 (2016)